Kinetics of Uropathogenic *Escherichia coli* Metapopulation Movement during Urinary Tract Infection

Matthew S. Walters,[a] M. Chelsea Lane,[b] Patrick D. Vigil,[a] Sara N. Smith,[a] Seth T. Walk,[c] and Harry L. T. Mobley[a]

Department of Microbiology and Immunology, University of Michigan Medical School, Ann Arbor, Michigan, USA[a]; Department of Genetics, University of North Carolina School of Medicine, Chapel Hill, North Carolina, USA[b]; and Department of Internal Medicine, Division of Infectious Diseases, University of Michigan Medical School, Ann Arbor, Michigan, USA[c]

ABSTRACT **The urinary tract is one of the most frequent sites of bacterial infection in humans. Uropathogenic *Escherichia coli* (UPEC) strains are the leading cause of urinary tract infections (UTIs) and are responsible for greater than 80% of uncomplicated cases in adults. Infection of the urinary tract occurs in an ascending manner, with colonization of the bladder leading to possible kidney infection and bacteremia. The goal of this study was to examine the population dynamics of UPEC *in vivo* using a murine model of ascending UTI. To track individual UPEC lineages within a host, we constructed 10 isogenic clones of UPEC strain CFT073 by inserting unique signature tag sequences between the *pstS* and *glmS* genes at the attTn7 chromosomal site. Mice were transurethrally inoculated with a mixture containing equal numbers of unique clones. After 4 and 48 h, the tags present in the bladders, kidneys, and spleens of infected mice were enumerated using tag-specific primers and quantitative real-time PCR. The results indicated that kidney infection and bacteremia associated with UTI are most likely the result of multiple rounds of ascension and dissemination from motile UPEC subpopulations, with a distinct bottleneck existing between the kidney and bloodstream. The abundance of tagged lineages became more variable as infection progressed, especially after bacterial ascension to the upper urinary tract. Analysis of the population kinetics of UPEC during UTI revealed metapopulation dynamics, with lineages that constantly increased and decreased in abundance as they migrated from one organ to another.**

IMPORTANCE **Urinary tract infections are some of the most common infections affecting humans, and *Escherichia coli* is the primary cause in most uncomplicated cases. These infections occur in an ascending manner, with bacteria traveling from the bladder to the kidneys and potentially the bloodstream. Little is known about the spatiotemporal population dynamics of uropathogenic *E. coli* within a host. Here we describe a novel approach for tracking lineages of isogenic tagged *E. coli* strains within a murine host by the use of quantitative real-time PCR. Understanding the *in vivo* population dynamics and the factors that shape the bacterial population may prove to be of significant value in the development of novel vaccines and drug therapies.**

Received 16 December 2011 **Accepted** 27 December 2011 **Published** 7 February 2012

Citation Walters MS, et al. 2012. Kinetics of uropathogenic *Escherichia coli* metapopulation movement during urinary tract infection. mBio 3(1):e00303-11. doi:10.1128/mBio.00303-11.

Invited Editor Jeff Miller, UCLA School of Medicine **Editor** Jeff Miller, UCLA School of Medicine

Address correspondence to Harry L. T. Mobley, hmobley@med.umich.edu.

In healthy adults, the urinary tract is a sterile environment. However, it is also one of the most common sites of bacterial infection in humans. It has been estimated that 40 to 50% of adult women will have experienced at least one urinary tract infection (UTI) in their lifetime, with many experiencing recurrent UTIs (1). During the year 2000, for example, UTIs resulted in an estimated 8.2 million physician visits, 1.7 million emergency room visits, and 366,000 hospitalizations of men and women, with an annual projected cost of more than $3.4 billion (2). The extraintestinal pathogen uropathogenic *Escherichia coli* (UPEC) was found to be the primary cause of community-acquired UTI, in as many as 80 to 90% of cases, and accounts for approximately 40% of nosocomial UTIs (3, 4). Frequently, UPEC strains that colonize the urinary tract of a patient can also be sampled from the patient's gastrointestinal tract, suggesting that the UPEC strains may originate from the patient's own intestinal flora (5). Transmission of UPEC may also occur via ingestion of contaminated food (6), sexual transmission (7, 8), and has even been suggested to occur person-to-person in the absence of sexual contact (9). Up to 95% of UTIs progress in an ascending manner, beginning with bacterial colonization of the periurethral area followed by infection of the bladder, leading to the development of cystitis. Bacterial ascension of the ureters may then lead to kidney infection (pyelonephritis), and dissemination from the kidneys to the bloodstream (bacteremia) may occur if the infection is left untreated (10, 11). Between 15% and 50% of patients with symptomatic acute cystitis also develop acute pyelonephritis, and approximately 12% of these patients develop subsequent bacteremia (12).

Bacterial ascension to the upper urinary tract is a complex process. While in the bladder, UPEC is capable of invading the cytoplasm of superficial facet cells and creating clusters of rapidly growing bacteria termed intracellular bacterial communities (IBCs) (13, 14). IBCs are thought to aid bacteria in evasion of the immune system and serve as a reservoir for subsequent UTIs. Planktonic bacteria allow the spread of bacteria away from the bladder. Bacteria must first ascend the ureters against the flow of

urine in order to colonize the kidneys and potentially gain access to the host bloodstream. All of this takes place while bacteria attempt to avoid the host immune response. Thus, the ureters and the kidney epithelial and capillary endothelial cell layers that separate the kidney from the bloodstream may act as barriers for ascending infection. The importance of flagellum-mediated motility for ascension of UPEC to the upper urinary tract and dissemination into the bloodstream, as well as for the maintenance of persistent infection, has been well established (15–17). However, compared to that seen with bacteria cultured *in vitro*, transcription of genes related to flagellum-mediated motility and chemotaxis was previously shown to be generally downregulated in an experimental mouse model of ascending UTI over a 10-day period (18) and in urine recovered from 8 women with UTI caused by *E. coli* (19). Given these data, it seems likely that expression of flagellar proteins occurs in only a single clonal subpopulation of bacteria at any given time. If this hypothesis were true, then clonal expansion of motile UPEC lineages in the bladder would facilitate ascension of one or both of the ureters and entry into the kidney. Since both kidneys and the spleen can become highly colonized over time in a patient with an untreated UTI, there is a strong possibility that multiple rounds of ascension and dissemination of clonal motile bacterial subpopulations arise.

The aim of this study was to systematically examine the *in vivo* population dynamics of UPEC during ascension and dissemination in a murine model of UTI. To investigate the growth dynamics of UPEC within an animal host, we generated 10 unique isogenic clones of wild-type UPEC strain CFT073 by introducing random nucleotide signature tags into the genome by Tn*7* transposition. These tagged bacterial strains were phenotypically identical, each carrying a unique 40-bp DNA signature tag within a noncoding sequence of the chromosome at the *pstS-glmS* intergenic region. Tag-specific PCR primers allowed us to enumerate each unique lineage during experimental UTI by the use of quantitative real-time PCR (qPCR). Loss or depletion of a tagged strain served as an indication of bacterial death, while dissemination between organs was approximated by the number and amount of unique strains present within each of the organs. We found that kidney infection and bacteremia associated with UTI seem to be the result of multiple rounds of ascension and dissemination and not necessarily of the expansion of a single clonal UPEC lineage. The UPEC lineages also appeared to behave as a metapopulation during UTI, in that the abundance of each tag was continually being modified by bacterial replication and death as well as by migration of bacteria from one organ to another. The numbers of each tagged bacterial strain within the animal host became less even, with respect to the inoculum, as bacteria ascended the urinary tract and spread systemically. The numbers of tagged lineages also became less even as infection progressed over time in the same organ location.

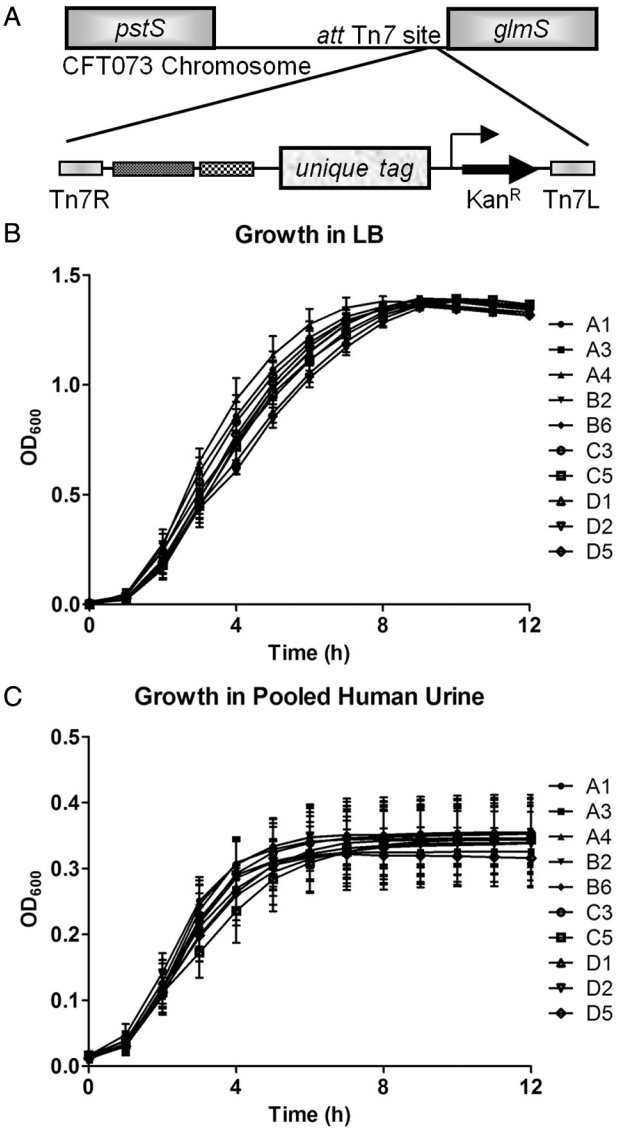

FIG 1 Construction of isogenic tagged *E. coli* CFT073 clones. (A) Tn*7* transposon carrying the unique tag inserts at the attTn7 site between the *glmS* and *pstS* genes of the *E. coli* CFT073 chromosome. (B and C) The tagged strains exhibited no differences in growth rates in either LB (B) or pooled human urine (C).

RESULTS

Growth and detection of tagged strains. To study the population kinetics of UPEC during ascending UTI in a host, we utilized a Tn*7* transposon to construct 10 uniquely tagged CFT073 clones. Insertion of Tn*7* transposons into the bacterial chromosome occurs at a high frequency near the end of the *glmS* operon (Fig. 1A) and at a lower frequency in other chromosomal sites (20, 21). Since Tn*7* inserts outside the actual *glmS* coding sequence, it should have no deleterious effects on host gene transcription. The tagged UPEC strains are genetically identical, with the exception of the 40-bp sequence in the transposon that serves as the unique tag. PCR was used to verify that the transposons carrying the 40-bp unique tags were inserted between the *glmS* and *pstS* genes at the high-frequency attTn7 attachment site (data not shown). To confirm that all of the tagged CFT073 strains were able to grow similarly, growth of each strain was measured over 12 h in both Luria-Bertani (LB) and sterile pooled human urine (Fig. 1B and C). As expected, all 10 UPEC lineages grew in LB and human urine at rates that were not significantly different.

C57BL/6J and CBA/J mice were infected with mixture of 1×10^8 bacteria containing equal amounts of each tagged strain. The typical colonization patterns observed at 4 and 48 h postinfection

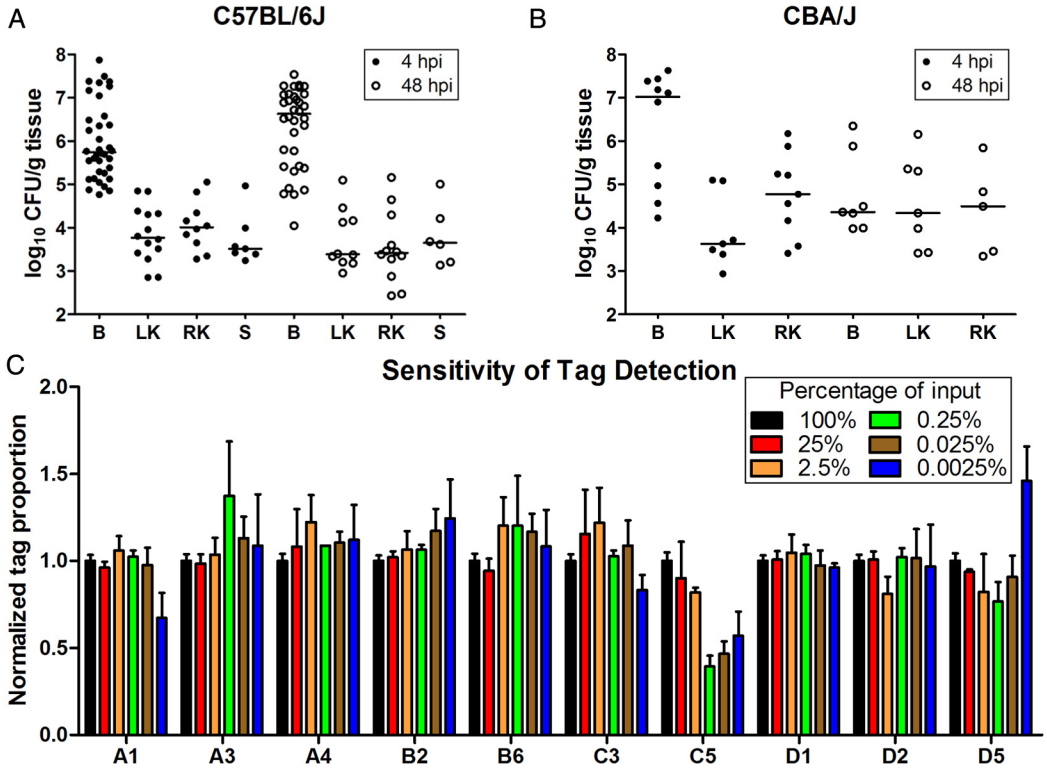

FIG 2 Levels of colonization in the mouse organs and *in vitro* verification of tag detection. (A and B) Typical colonization levels in the bladders, kidneys, and spleens of C57BL/6J mice (A) and bladders and kidneys of CBA/J mice (B) at 4 hpi and 48 hpi in mice infected with 1×10^8 *E. coli* CFT073. CBA/J mice exhibited a less robust level of bladder colonization at 48 hpi than the C57BL/6J mice. B, signifies bladder; LK, left kidney; RK, right kidney; S, spleen. (C) An inoculum sample was prepared, and equal volumes of undiluted and diluted samples were cultured on LB agar plates for genomic DNA extraction. The quantity of each tag was measured by qPCR and compared to the quantity of the specific tag in the inoculum (100%) sample normalized to 1. The sample diluted 25%, equivalent to the proportion of bacteria recovered from infected mouse organs in this study, did not significantly differ from the inoculum sample. Tag name is indicated along the x-axis.

(hpi) in the bladders, kidneys, and spleens of C57BL/6J mice are shown in Fig. 2A, while bladder and kidney bacterial loads for CBA/J mice are shown in Fig. 2B. At 48 hpi, C57BL/6J mice displayed a more robust bladder infection than CBA/J mice, with the strains showing similar levels of colonization at 4 hpi. CBA/J mice tended to have higher colonization in the kidneys. To determine the sensitivity of our assay measuring tag abundance, we combined equal numbers of the tagged CFT073 strains and cultured the same volume of undiluted (1×10^8 bacteria) and samples diluted to 25% (2.5×10^7 bacteria), 2.5% (2.5×10^6 bacteria), 0.25% (2.5×10^5 bacteria), 0.025% (2.5×10^4 bacteria), and 0.0025% (2.5×10^3 bacteria) of the original undiluted culture on selective LB agar plates. Bacteria were washed from the entire plate, and genomic DNA (gDNA) was extracted from a portion of the sample. The relative quantities of the tags, as measured by qPCR, in the diluted samples were then compared to the abundance of each specific tag in the undiluted sample normalized to 1 (Fig. 2C). The sample containing 25% of the total bacteria present in the original culture, equivalent to amount of bacteria used in our *in vivo* experiments, yielded an accurate representation of the abundance of each tag present in the 100% (undiluted) sample. More variation in the quantities of each tag was observed as the samples became more diluted, resulting in some tags being overrepresented or underrepresented in the samples containing a fraction of the bacterial population in the undiluted culture.

The population of tagged strains does not remain homogeneous during experimental infection. Quantitative real-time PCR was used to determine the presence of each tag and relative tag abundances in each of the organs tested at 4 and 48 hpi. We first examined how many tags were present in the organs, regardless of their relative quantities. Two different mouse backgrounds, C57BL/6J and CBA/J, were used in these studies. C57BL/6J is the most widely used inbred strain and was the first mouse strain to have its genome sequenced (22), while CBA/J mice have been used extensively in the ascending UTI model (18, 23–26).

At 4 hpi, 13/15 (~87%) of C57BL/6J mice and 9/15 (~60%) CBA/J mice had detectable levels of all tags in their bladders (Fig. 3). Two C57BL/6J mice and six CBA/J mice lost at least one of the tagged strains in the bladder population at this time point, signifying that death or loss of clonal lineages occurs early after infection in the murine model and has the potential to alter the population structure. The tagged CFT073 strains were able to reach both the kidneys and the bloodstream, as measured by bacteria in the spleen, by 4 hpi. Also at 4 hpi, the number of tags detected decreased as bacteria ascended the urinary tract compared to the number present in the bladder in both mouse lines, suggesting that the ureters and epithelial and endothelial barriers separating the kidney tubules from the bloodstream represented significant barriers to the invading bacteria. Mice sacrificed at 48 hpi displayed even fewer organs containing all of the tags present in the initial inoculum. Only 3 of the 14 (~21%) bladders from C57BL/6J mice and 2 of 15 bladders (~13%) from CBA/J mice contained detectable levels of all tags (Fig. 3). The kidneys and

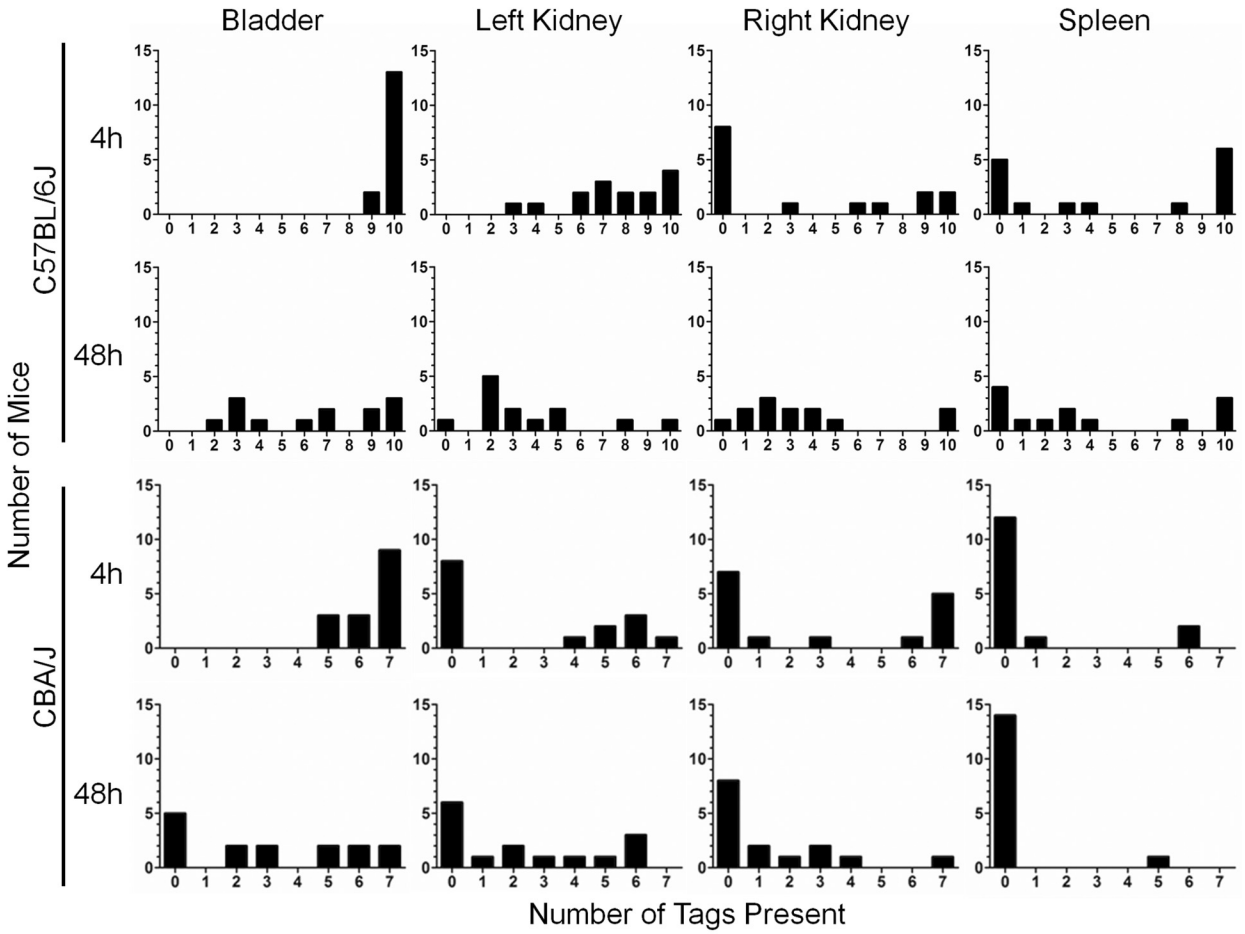

FIG 3 Frequency of tagged strains recovered from the bladder, left kidney, right kidney, and spleen in C57BL/6J and CBA/J mice. Detectable levels of most tags were found in bladders at 4 hpi. The number of unique tags found decreased in the kidneys and spleen and as infection progressed over time.

spleen also contained fewer tags in the bacterial population compared to the same organs at 4 hpi.

Patterns of tag distribution during ascending infection. Throughout the course of these infections, we observed several patterns of tag prevalence during bacterial challenge of the mouse urinary tract. The percentage of each tag in an infected organ from C57BL/6J and CBA/J mice is shown in Fig. 4. At 4 hpi and 48 hpi, we found 5 C57BL/6J mice that contained all or most ($\geq$8) of the uniquely tagged UPEC strains in the bladder, left and right kidneys, and spleen at approximately the same proportions (Fig. 4A—mice 1, 11, 14, 15, and 28). Mice sacrificed at the later time point most often displayed bacterial populations composed mainly of 2 to 4 dominant tags, suggesting that host environment factors (such as physical barrier of entry into the ureter, mechanical barriers due to the flow of urine, and neutrophil infiltration as part of the immune response) caused the population to become more homogenous and less diverse over time.

The tag profile of the bacterial clones in the spleen would oftentimes closely resemble the tagged lineages observed in one of the kidneys, as would be expected, since the most numerous clones of uniquely tagged bacteria in the kidney would have the greatest chance of breaching the 2 cell layers between the kidneys and bloodstream. However, this was not always the case. In some instances, we found tagged clones of bacteria in the kidney or spleen that were not detected in the bladder or kidneys, respectively, organs through which the bacteria would have had to travel in order to ascend the urinary tract (Fig. 4A, mouse 24; Fig. 4B, mice 13, 14, 15, and 17). These results imply that some bacterial lineages are able to ascend the urinary tract but may not persist in all locations of the urinary tract or persist only as a very small minority of the population. In the experiment involving CBA/J mice, the CFT073 strain carrying tag D2 appeared to dominate in many of the mice at both 4 and 48 hpi. However, the experiments involving the C57BL/6J mice, which included data from 5 separate inocula and infections, did not exhibit a bias towards the strain carrying tag D2. Thus, the domination of tag D2 in CBA/J mice was likely a random event that might have diminished if more CBA/J experiments were performed.

The effect of individual tags and location on the bacterial population. To explore whether experimental infection resulted in differences in the overall abundance of UPEC clones, we conducted a two-way analysis of variance (ANOVA) of the normalized proportion of each tagged clone in the bladder, left kidney, right kidney, and spleen during ascending UTI in C57BL/6J and CBAJ mice (Fig. 5). The variation in tag abundance was greater at the 48-h time point (Fig. 5B and D) than at the 4-h time point (Fig. 5A and

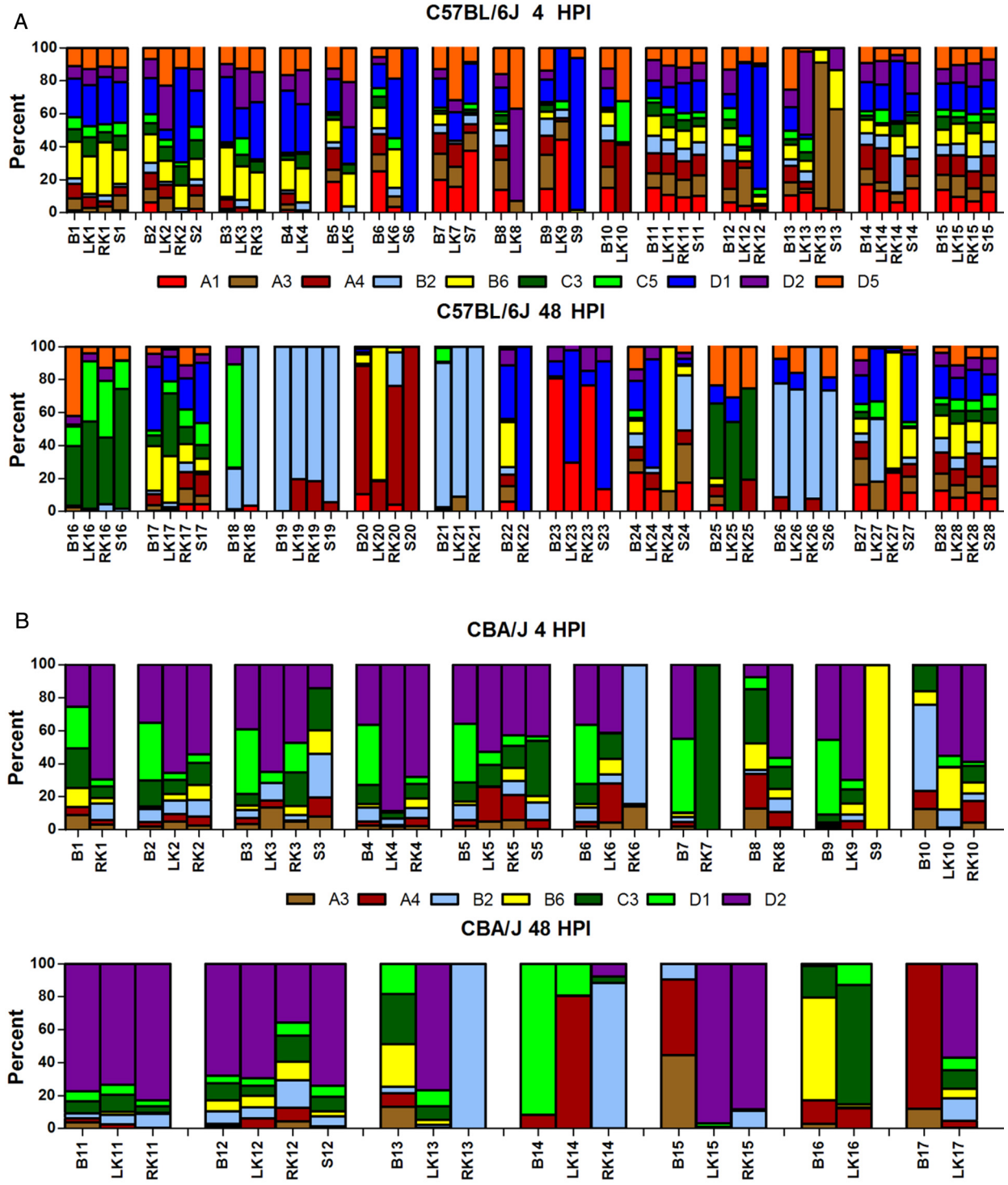

FIG 4 Quantification of unique tags in the bladder, left kidney, right kidney, and spleen at 4 hpi and 48 hpi for (A) C57BL/6J mice and (B) CBA/J mice. The relative quantities of each tag in all of the organs tested are shown. B, bladder; LK, left kidney; RK, right kidney; S, spleen (used as a proxy for systemic infection); each number indicates a specific mouse. A total of 10 tags were used in experiments involving C57BL/6J mice, while 7 tags were used with the CBA/J mice. Results for the organs from each mouse are grouped together.

C) and was also greater in CBA/J mice than in C57BL/6J mice. Subtle but significant differences in tag abundance were seen in C57BL/6 mice at 4 h, but no significant differences were seen at 48 h, suggesting that initial differences in abundance are not maintained throughout infection. A similar trend was observed in CBAJ mice, although the abundance of at least one tag remained

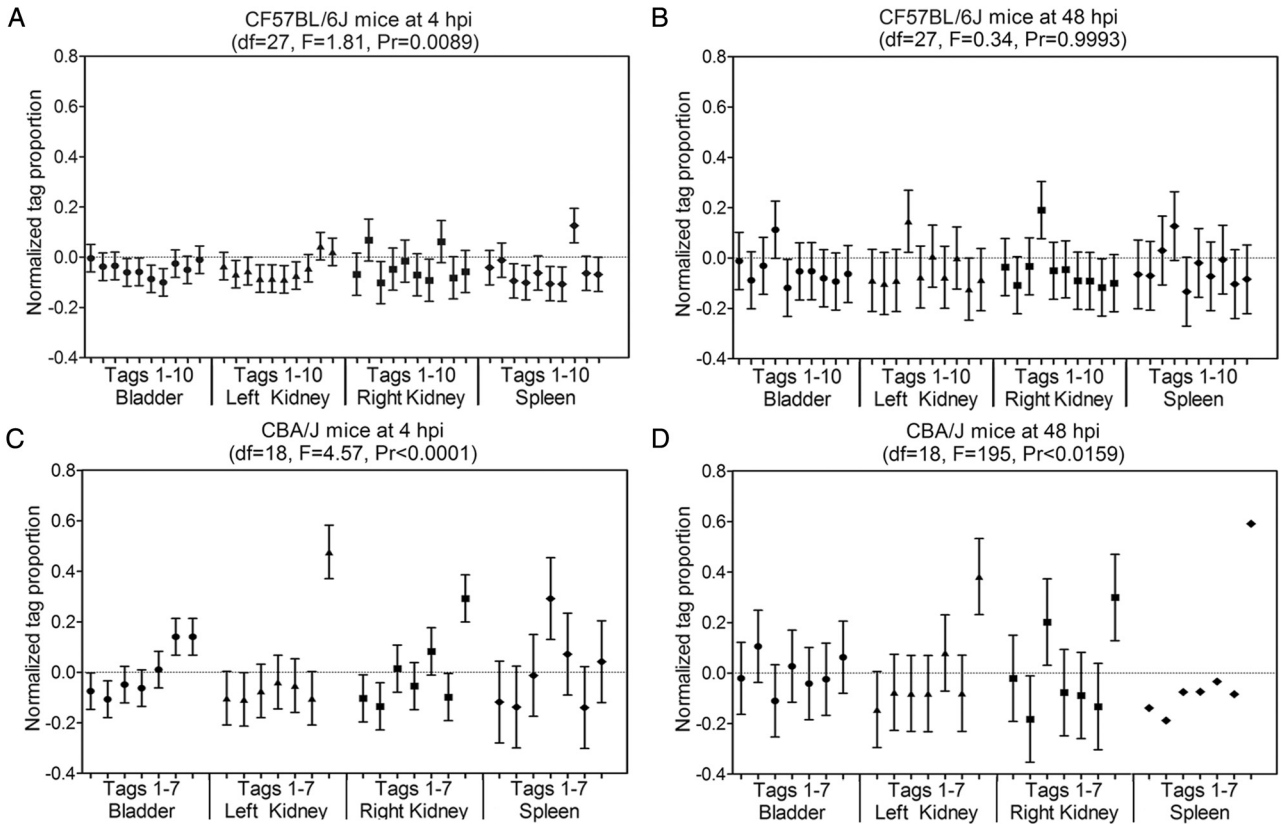

FIG 5 Two-way analysis of variance (ANOVA) of the organ determined by tag effect on the normalized tag proportion. Data for bladders (circles), left kidneys (triangles), right kidneys (squares), and spleens (diamonds) are shown. (A and B) Data for C57BL/6J mice at 4 hpi (A) and 48 hpi (B) show increasing variability in tag distribution in the bacterial population as infection progressed. The order of A1, A3, A4, B2, B6, C2, C5, D1, D2, and D5 for the 10 tags is maintained between organs. (C and D) Data for CBA/J mice at 4 hpi (C) and 48 hpi (D) displayed greater variation at both time points, but the trend of increasing tag disproportion as infection progressed remained. The order of A3, A4, B2, B6, C2, D1, and D2 for the 7 tags is maintained between organs. There are no error bars for the 48-hpi CBA/J spleen result, because only 1 mouse had a systemic infection at that time point.

significantly different at 48 h. Despite the increased variance present in the experiments performed with the CBA/J mice, the tagged populations still became less even compared to the inoculum as they ascended the urinary tract and over time.

Population evenness decreases during ascension of urinary tract and over time. Since the total numbers of uniquely tagged bacteria in each group differed slightly in different experimental inocula, as determined by qPCR, we normalized data so that the results from the experiments could be directly compared. To accomplish this, data for each organ were normalized so that the quantity of each tag relative to other tags in the same sample was represented as the absolute value of the difference between the inoculum and data point at either 4 or 48 hpi. The proportion for a tag in a given organ was expressed as $|l_n - O_n|$ (where n represents the tag number n, l is the input percentage of tag number n, and O equals the output percentage of tag number n). The equation $\Sigma_{i=1}^{n} |l_n - O_n|$ yields an average distance each tag moved away from the amount of the tag in the input over the course of the experiment. The maximum distance a sample could change was calculated with the assumption that complete dominance would result in one tag being present at 100% of the recovered tags and all other tags at 0% of the total population. The distance measure of each sample was divided by the maximum distance measure to generate an estimation of sample evenness.

These values closely paralleled Pielou's evenness index; for simplicity, only the latter is reported (Fig. 6). Pielou's evenness index indicates how close the population number of each species (isogenic tagged clones) is to that of another. The values are constrained between 0 and 1, with a community being represented as more even as the value approaches 1. A decrease in evenness was observed in comparing clones from the input, bladder, kidney, and spleen samples in each experiment at both time points. Evenness of tagged lineages in C57BL/6J and CBA/J bladders and kidneys decreased significantly from 4 hpi to 48 hpi (C57BL/6J bladder and kidney, $P \leq 0.001$; CBA/J bladder and kidney, $P \leq 0.05$ and $P \leq 0.01$, respectively). Clones present within the spleen at 4 hpi contained exceedingly uneven combinations of tags that did not change significantly between 4 hpi and 48 hpi. The lack of population evenness observed in the spleen samples represented some of the most extreme measures recorded. The 10 tagged CFT073 strains used in these studies were also cultured *in vitro* in LB broth and subjected to passage every 8 or 16 h for 48 h. The tagged strains cultured in LB did not demonstrate the dramatic changes in population evenness that were observed *in vivo* using the murine model of ascending UTI, suggesting that the host environment drives change in tag abundance. The results of *in vitro* culture experiments further substantiate the lack of any growth rate defect in any of the tagged strains (Fig. 1B and C).

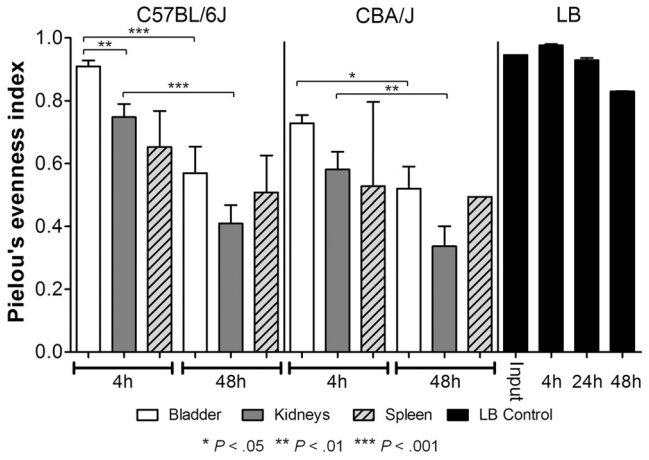

FIG 6 Pielou's evenness index for data from C57BL/6J and CBA/J mice demonstrates that population evenness decreased as a function of both time of infection and ascension from the bladder to the kidneys and bloodstream. When the tagged strains were cocultured in LB and sampled at 4 h, 24 h, and 48 h, the populations remained more even and closely resembled the input population.

Examination of nonmetric multidimensional scaling (nMDS) and principal components analysis (PCA) plots of the data revealed that the presence and abundance of a specific tagged UPEC strain at a given organ site appeared to occur randomly (Fig. 7; Table 1 and 2). The goal of these unconstrained ordination analyses was to extract gradients of greatest variation from the samples and define similarities and dissimilarities in the data. PCA converts correlated variables into principal components (uncorrelated variables) that explain the total variance in a data set, with the first principal component accounting for as much of the variability as possible and each subsequent component accounting for each subsequent greatest variance. nMDS approximates a nonlinear transformation of the pattern of proximities within a data set, while preserving the given order and remaining monotonic. It provides a visual representation of the similarities or distances among the data. These tests revealed a radial star pattern, with each arm representing samples dominated by a specific tag. Each arm consisted of a mixture of bladder, left and right kidney, and spleen samples, oftentimes from different mice, illustrating that a particular tag did not have a consistent advantage in a single animal or specific organ site (Fig. 7).

The PCA plots containing the first 2 principal components define in 2-dimensional space where the largest variance in the data set lies. Data for C57BL/6J mice and CBA/J mice are shown in Fig. 7A and B, respectively. PCA plots are susceptible to the arch effect (a U-shaped line of sample points) when applied to data that follow a gradient in which there is a progressive turnover of dominant variables; this artifact is observed in these graphs. However, PCA was still useful when examining each vector loading value (the Eigen vector coefficient) and Eigen value to identify which tag dominated each of the vectors. Eigen values represent the amount of variation captured by each principal component, while Eigen vectors act as weighting coefficients and represent the contribution of each variable to the principal components. The Eigen values and Eigen vectors for the C57BL/6J mice and CBA/J mice are listed in Table 1 and 2, respectively. These values depict which tag dominated in each of the vectors (axes). Each tag dominated only one axis (or principal component), with the exception of the D2 tags, which showed the most variation in the PC8 and PC10 axes of the data from the C57BL/6J mice, and D5, which did not dominate any axis in the C57BL/6J experiments.

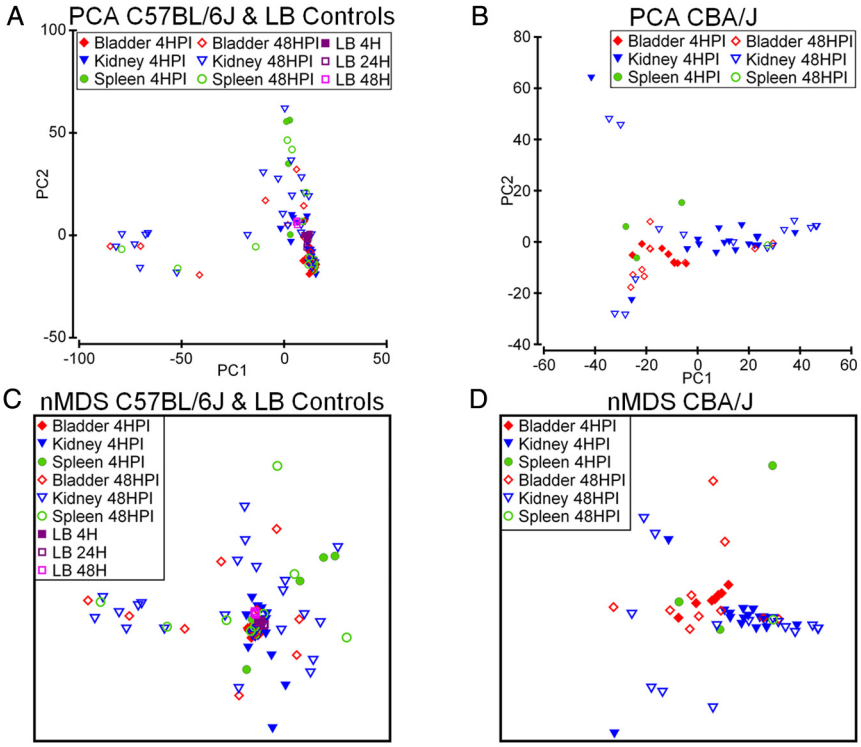

FIG 7 Multivariate analysis of UPEC reveals that the bacterial lineages behave as a metapopulation in the murine host, with bacterial replication, death, and migration between infection sites all influencing population dynamics. (A) PCA of C57BL/6J mice by the use of normalized tag proportions to compare the clones between experiments. (B) PCA of CBA/J mice by the use of normalized tag proportions to compare the clonal lineages between experiments. (C–D) nMDS using 100 iterative restarts of C57BL/6J and CBA/J data, respectively. Closed symbols represent data from 4 hpi, and open symbols signify 48 hpi. The data from the bladders at 4 hpi group together, and the bladders contained lineages of bacteria that more closely resembled the input. The kidneys at 4 hpi exhibited slightly more clonal diversity than the bladders at the same time point. By 48 hpi, clones in these organs became more diverse, resulting in spread of the data points. Populations in the spleen at both 4 hpi and 48 hpi displayed greater diversity. These effects were not observed in bacteria grown *in vitro* in LB at 4 h, 24 h, or 48 h, resulting in the clustering of these data points with the bladder data at 4 hpi.

Nonmetric multidimensional scaling plots for C57BL/6J mice (Fig. 7C) and CBA/J mice (Fig. 7D) also depict a radial star pattern. Note that, because this analysis maximizes the spaces on the graph, distances between data points can be compared only to other points on the same graph. Data points for tags in the bladder and kidneys in both mouse strains at 4 hpi (closed symbols) cluster

TABLE 1 Eigen vectors and Eigen values from C57BL/6J principal components analysis[a]

	Eigen vector or value									
Tag or parameter	PC1	PC2	PC3	PC4	PC5	PC6	PC7	PC8	PC9	PC10
A1	-0.112	0.127	-0.196	-0.128	0.218	0.717	0.595	-0.008	0.032	-0.016
A3	-0.035	0.02	0.02	-0.012	0.211	0.555	-0.759	-0.258	0.049	-0.026
A4	-0.063	0.429	-0.701	-0.255	0.339	-0.332	-0.111	-0.122	-0.052	0.009
B2	-0.979	-0.143	0.065	0.042	0.047	-0.107	-0.012	-0.026	0	-0.027
B6	-0.119	0.285	-0.356	0.156	-0.836	0.199	-0.098	0.032	-0.054	-0.046
C3	0.03	0.117	-0.089	0.883	0.232	-0.014	0.089	-0.207	-0.297	0.07
C5	-0.015	0.135	-0.027	0.227	0.006	-0.051	0.03	-0.065	0.884	0.375
D1	-0.077	0.814	0.557	-0.061	0.039	-0.037	0.012	0.037	-0.049	-0.104
D2	-0.052	0.062	-0.034	0.011	0.094	0.109	-0.159	0.677	-0.233	0.659
D5	0.006	0.01	-0.135	0.239	0.169	0.032	-0.116	0.641	0.255	-0.637
% variation (Eigen value)	39.6	18.4	10.5	8.9	6.7	5.0	3.8	3.3	2.3	1.5

[a] Eigen vectors represent a component of the inherent variability in a data set. Eigen values represent the variance of the data contained in each principal component. PC, principal component.

towards the middle of the plots and are similar to those determined for the inoculum. At 48 hpi (open symbols), the bladder and kidney data points spread out as the populations of tagged strains became less even. Data points for the spleen are more spread out at both 4 and 48 hpi, suggesting that traveling from the kidney to the bloodstream represents a significant barrier to invading bacteria in an ascending UTI. The data for the *in vitro* LB cocultures of the 10 tags group together in the center of the C57BL/6J plot and do not spread out over time, and the tag distribution in the population remained quite even over the course of the experiment.

DISCUSSION

In this study, we constructed 10 isogenic uniquely tagged clones of UPEC strain CFT073 (Fig. 1A), a prototypical pyelonephritis strain, and followed the presence of these tagged strains through ascension of the urinary tract over time using qPCR. Since bacteria were recovered from infected organs on LB agar, the resulting lineages of tagged strains were amplified following growth on these plates. This, coupled with the use of qPCR to enumerate the quantity of each tag in the sample, allowed us to develop an exquisitely sensitive assay to track the population dynamics of UPEC in an ascending UTI.

Analysis of the *in vivo* clones of *E. coli* CFT073 by the use of a murine model of ascending UTI revealed that the mixtures of tagged strains contained bacteria of equal fitness. The strains displayed no growth differences during culture in either LB or pooled human urine (Fig. 1B and C), which was expected, since the strains differed only by the unique 40-bp nucleotide tag. Early during acute UTI, most of the tagged clones were still detected in the bladder, with fewer present in the kidneys and bloodstream (Fig. 3). Even though most of the tagged lineages were present at this early time point, their relative proportions, compared to the input population, were already being altered (Fig. 4). These effects were magnified at the 48 h time point. Several tags were not detected in organs recovered from infected mice at this time point, and it was generally found that one or two tagged lineages composed the majority of the entire bacterial population. These results argue that a series of stochastic events occurs once bacteria colonize the host, leading to a small number of tags or a single tag (clone) of bacteria dominating in a given organ site. Other lineages decreased in size and likely become lost from the population. The events leading to these effects occurred earlier in the infection cycle than expected, taking place as soon as 4 h after the host became colonized by the pathogen. As infection in the murine host progressed, the abundance of tagged lineages diverged from the level in the inoculating population.

A recent study using a mixture of 40 isogenic tagged bacterial strains and multiplex PCR also examined the population dynamics of UPEC as it related to the formation of intracellular bacterial communities in mice with UTIs (27). Schwartz and colleagues proposed that a series of bottlenecks exists in the bladder and kidneys, with the most stringent occurring within the first 24 h of their experimental UTI model using C3H/Hen mice. It was found that IBC formation in a host cell derived from a single bacterium and that less than 0.002% of the inoculum was able to form IBCs,

TABLE 2 Eigen vectors and Eigen values from CBA/J principal components analysis[a]

	Eigen vector or value						
Tag or parameter	PC1	PC2	PC3	PC4	PC5	PC6	PC7
A3	0.012	0.074	0.113	-0.01	-0.119	-0.095	-0.979
A4	-0.133	-0.224	-0.062	0.908	-0.141	-0.29	0.011
B2	-0.166	-0.403	-0.822	-0.163	0.277	-0.088	-0.151
B6	-0.078	-0.036	-0.279	-0.144	-0.934	0.13	0.066
C3	-0.294	0.856	-0.34	0.078	0.051	-0.234	0.037
D1	-0.123	-0.166	0.211	-0.343	-0.108	-0.878	0.112
D2	0.92	0.142	-0.263	0.068	-0.046	-0.238	0.02
% variation (Eigen value)	38.9	16.0	12.5	11.4	9.2	7.0	5.0

[a] Eigen vectors represent a component of the inherent variability in a data set. Eigen values represent the variance of the data contained in each principal component. PC, principal component.

creating a "founder effect" for the ensuing UTI. The use of 40 tagged strains in that study allowed the authors sensitivity in detecting the loss of a given tag. However, the multiplex PCR assay was capable of detecting the presence or absence of the tags only in bladder or kidney populations, without regard to the relative abundance each tag represented in the whole population. Our present report adds a new dimension to our understanding in that the qPCR results presented here precisely measure the proportion that each tag contributes to the population and allow analysis of entire bacterial populations in the bladder, kidneys, and spleen (bloodstream) of infected mice.

The ascension from bladder to kidney does not appear to be the result of a single clone ascending the ureter and colonizing the kidney but rather the result of a large number of bacteria migrating together or in waves and reaching the kidney at nearly the same time. Further, the lineage that reaches one kidney may be distinct from the lineage that reaches the other kidney, as many mice with colonization of both kidneys were found to have different tags dominating each respective kidney at 4 and 48 hpi (Fig. 4). In contrast, the passage of invading UPEC into the bloodstream, as measured by levels of bacteria found in the spleen, was far less diverse. The major restriction point in bacterial population dynamics of an ascending UTI appears to be the transition from the urinary tract into the bloodstream. The results also demonstrate that UPEC reliably reached the bloodstream in less than 4 h after inoculation of the bladder, based on the number of mice with bacteria present in the spleen. No bacteria were found in kidneys immediately following inoculation, indicating that these results did not originate from vesicoureteral reflux at the time of inoculation (data not shown). The rapidity of the invasion of the bacterium into the bloodstream was greater than previously appreciated and is further substantiated by observations in human UTI patients. It has been shown that as many as half of patients who present with signs and symptoms of pyelonephritis caused by UPEC have documented bacteremia at the time of initial presentation (28).

Based on PCA and nMDS analysis, our results imply a model involving distinct metapopulations of UPEC as bacteria ascend and move through the host urinary tract and disseminate into the bloodstream. The term metapopulation was originally introduced by Levins in 1969 to describe a "population of populations" connected by migration (29). The perseverance of these populations represents a balance between local extinctions and recolonization to establish new populations at unoccupied sites (30). Multivariate analyses of the data reveal that UPEC migration appears to occur between the kidney and the bladder, with bacteria ascending the ureter to the kidneys, as well as being carried by the flow of urine back towards the bladder. In contrast, movement from the kidneys to the bloodstream seems to represent more of a classical bottleneck in the infection. In addition to flux between sites, normal ecological processes shape the bacterial community at a given site. Forces such as resource competition, growth, and bacterial death from immune-mediated processes operate at each site. If movement between sites were the main factor in the population dynamics of infecting bacteria, then the populations would be expected to become more homogeneous over time. However, if local processes such as bacterial replication and death play a greater role, then the populations would begin to diverge from the initial population. Bacterial populations in both strains of mice became less even as bacteria ascended the urinary tract and over time. The data presented here suggest that flux is sufficient to establish the different populations in less than 4 hpi, but since the populations do diverge and become less even over time and space, local forces appear to dominate over the course of infection, creating distinct populations at 48 hpi that bear little resemblance to the populations present in the inoculum. The use of two host backgrounds allowed us to examine whether there were any specific host effects on the bacterial population dynamics. The C57BL/6J mice and CBA/J mice displayed similar patterns of UPEC population dynamics (Fig. 5 and 6), though the CBA/J mice displayed more variance than the C57BL/6J mice. The CBA/J mice also exhibited slightly different patterns of infection compared to the C57BL/6J mice (Fig. 2A and B), suggesting that minor differences may exist between the progressions of experimental UTIs in these two strains.

The host urinary tract presents many challenges that invading bacteria must overcome to persist. Urine flow and exfoliation of the umbrella cells lining the bladder represent physical mechanisms that UPEC must evade to colonize the urinary tract (31–33). UPEC are also subjected to a robust infiltration of host inflammatory cells, composed mainly of neutrophils (24, 34), as well as antimicrobial peptides in the bladder and kidneys (35), in response to infection of the urinary tract. The outcomes of these interactions, along with nutrient availability, have a substantial impact on the population of bacteria colonizing the urinary tract. The change in tag abundance observed in these experiments seems most likely to be the result of genetic drift within the tagged clones and bottlenecks encountered during ascending UTI. Genetic drift in a population operates randomly and occurs by chance. Since not all cells of a clone experience the host environment in precisely the same manner, gene expression within the clones may differ. If a clone is able to begin expressing a factor based on sensing a signal before other clones, such expression may provide an advantage to the clone and lead to expansion of that lineage. An example of this may be type 1 fimbriae, which attach to mannose moieties of uroplakin receptors on cells lining the bladder and are subject to phase-variable expression (36, 37). A bacterium that is already expressing type 1 fimbriae would be primed to bind host bladder cells and resist being lost through the action of urine flow. As a result, clones from this lineage might become more abundant with respect to the other tagged lineages present during infection.

Given that UPEC strain CFT073 is a virulent uropathogen isolated from the blood of an infected human patient and the relatively short time course of the experiment, it would be expected that beneficial mutations due to selection pressure from the host would occur at a low frequency. UPEC is already adapted to life in the urinary tract of a host, making the chance of a mutation incurring a large fitness advantage low, since such mutations have already become fixed in the population. Future experiments examining the effects of evolutionary adaptation to the host by passage of a tagged clone through an ascending UTI model multiple times and comparing the relative fitness of that strain to the fitness of other tagged strains that have not been previously subjected to passage may reveal novel factors arising from small beneficial mutations that confer advantages during colonization of the host. Understanding the population dynamics of an ascending UTI may help identify steps in the pathogenic cascade critical to shaping the bacterial population in the host. The changes in bacterial populations during infection that allow some lineages to become dominant and others to be lost may represent novel targets for the development of new therapeutics to treat UTIs.

TABLE 3 Primers used in qPCR studies and cloning

Primer name	Sequence (5'–3')
qPCR A1	TTCCCGAGCGCACCACAAA
qPCR A3	ACACATACATCTCGCACGCAAACG
qPCR A4	TTAGCACGCACTCCCACCACCAA
qPCR B2	TTAGCACGCACTCCCACCACCAA
qPCR B6	AAACCAACATCTCCCTCGCCC
qPCR C2	TTCTACCACGCCCAAACATCACC
qPCR C5	ATAACACTCCCGCCCACGAGAA
qPCR D1	ACACAGCAAACGCCAGCTCTAT
qPCR D2	TTCGAACTCGACCGCCAACCAAA
qPCR D5	CCACTCAATCACGCAACACCC
pWAM qPCR F1	TTTGAGACACAACGTGGCGGAT
P2	ATCTCCACTAGTTACCTACAACCTCAAGCT
P4	CTGCAAACTAGTTACCCATTCTAACCAAGC

MATERIALS AND METHODS

Bacterial strains, plasmids, and culture conditions. UPEC strain CFT073 is a prototypical uropathogenic strain isolated from the blood and urine of a hospitalized patient with acute pyelonephritis (38). A nalidixic acid-resistant (Nal^r) mutant of CFT073 was used as the parental strain for creation of the tagged UPEC lineages. The pathogenesis of the CFT073 Nal^r mutant has been previously shown to be indistinguishable from that of wild-type CFT073 (39). All strains were cultured aerobically at 37°C on Luria-Bertani (LB) agar plates or in LB broth with appropriate antibiotics. Antibiotics for selection were used at the following concentrations: ampicillin (Amp), 100 μg/ml; kanamycin (Kan), 25 μg/ml; chloramphenicol (Cam), 20 μg/ml; and Nal, 15 μg/ml.

Construction of isogenic tagged *E. coli* cft073 strains. The unique tags used in these studies were amplified from pUT/mini-Tn5Km2 (40) by the use of primers P2 and P4 (Table 3). PCR products of the unique tags were digested with SpeI and cloned into the SpeI site of plasmid pCIITn7K-a (41), which features a mini-Tn*7* transposon with kanamycin and chloramphenicol resistance markers. The resulting plasmids were transferred to the mating *E. coli* S17 λpir strain by electroporation. Uniquely tagged isogenic clones of *E. coli* CFT073 were created using a modified triparental mating method as described by Bao et al. (42). Briefly, *E. coli* strain S17 λpir bacteria containing the Tn*7* transposon and unique tags were used as donors, Nal^r *E. coli* CFT073 was used as the recipient, and *E. coli* K-12 carrying plasmid pUX-BF13 (42) served as the helper strain. The pUX-BF13 helper plasmid expresses the Tn*7* transposase that leads to the insertion of the kanamycin resistance gene and unique tags located between Tn7R and Tn7L into the chromosome at the attTn7 attachment site between the *pstS* and *glmS* genes (20). The three strains were incubated together on LB agar plates containing no antibiotics for approximately 16 h at 30°C. Bacteria from the mating plates were streaked for isolation and patched onto LB agar plates containing appropriate antibiotics. Clones that were Nal^r, Kan^r, Amp^s, and Cam^s were selected for PCR verification of tag insertion at the attTn7 attachment site.

Recombinant DNA techniques. Plasmid purification, PCR, ligation, restriction digest, transformation, and DNA gel electrophoresis were performed using standard methods (43). DNA concentration and purity were measured using a NanoDrop ND-1000 spectrophotometer (Thermo Scientific). DNA sequence analysis was carried out at the University of Michigan Biomedical Research DNA Sequencing Core using an Illumina IIx Genome Analyzer.

Experimental murine model of ascending UTI. Mice were infected as previously described (24, 44) with modifications. Briefly, overnight cultures of the relevant strains were adjusted to an estimated density of 4×10^9 CFU/ml and mixed equally. Six- to 8-week-old female CBA/J (the Jackson Laboratory, Bar Harbor, ME) or C57BL/6J (the Jackson Laboratory, Bar Harbor, ME) mice were anesthetized with ketamine-xylazine and transurethrally inoculated with a 25-μl bacterial suspension over a 30-s period, delivering approximately 1×10^8 CFU per mouse. Dilutions of the inoculum were made, and CFU were quantified using a Spiral Biotech Autoplate Spiral Plating system (Spiral Biotech, Norwood, MA) to determine the input CFU per milliliter. Mice were euthanized by an overdose of isoflurane at 4 and 48 hpi. Animal protocols were approved by the University Committee on Use and Care of Animals at the University of Michigan Medical School.

gDNA extraction and quantitative real-time PCR. The bladders, left kidneys, right kidneys, and spleens from infected mice were removed and homogenized using 2 ml of sterile phosphate-buffered saline (PBS) and an Omni GLH homogenizer (Omni International). Twenty-five percent (500 μl) of each organ homogenate was plated and cultured on selective LB agar plates containing kanamycin. The majority of the resulting bacterial growth on the LB agar plates produced a lawn of bacteria that were washed from the agar using sterile PBS. At a minimum, 200 bacterial colonies per organ sample were taken from the LB agar plates using sterile PBS. Samples containing fewer than 200 bacterial colonies were discarded. The resulting bacterial suspensions, which contained a mixture of the tagged UPEC lineages, were adjusted to an optical density at 600 nm (OD_{600}) of 2.0. Genomic DNA (gDNA) was extracted from these samples by the use of a DNeasy blood and tissue kit (Qiagen) following the manufacturer's protocol for Gram-negative bacteria. All gDNA extractions were diluted to 10 ng/μl, split into aliquots, and stored at −20°C until use.

qPCR was performed using a Stratagene Mx3000P instrument. The primers used for qPCR are listed in Table 3. Each reaction utilized a primer common to all tags used in the study and a separate primer unique to each tag. All qPCRs were performed using a 20-μl reaction volume. Each reaction contained 10 μl of 2× SYBR green PCR master mix (Stratagene), 300 nM carboxy-X-rhodamine (ROX) passive reference dye, 150 nM (each) primer, and 50 ng of gDNA. No-template controls were used to confirm that reagents were not contaminated with gDNA, and melting curve analysis verified that no primer dimers were present. Standard curves, based on 10-fold dilutions ranging from 3×10^6 to 300 copies for the tag being quantified, were determined for each reaction plate and used to quantify the amount of each tag in a given sample. A standard curve with a slope of -3.3 ± 0.3 (90% to 110% efficiency) was considered acceptable. To verify that our method of bacterial growth and recovery accurately portrayed the true abundance of each tag, we performed an *in vitro* experiment combining equal amounts of each tagged strain and plating either an undiluted sample containing 1×10^8 bacteria or dilutions containing 25%, 2.5%, 0.25%, 0.025%, and 0.0025% of the original bacterial population. Bacteria from the entire plate surface were washed from the agar with sterile PBS, and gDNA was extracted from each sample. The resulting quantities of each tag in the diluted samples were then determined and compared to the quantities of each tag in the undiluted sample.

qPCR data and statistical analysis. To test for differences in the abundances of tagged CFT073 clones in the urinary tracts of mice, we conducted a two-way analysis of variance (ANOVA) using the general linear model procedure (PROC GLM) and SAS statistical software (SAS Institute, Cary, NC). Briefly, the abundance of each tag was estimated according to the proportions of the individual tags by the use of qPCR (copy number of each tag/total number of copies of all tags). Tag proportions were normalized to the total copy number of the input inoculum (proportion of tag — proportion of input inoculum). This variable, called the normalized tag proportion, was used as the dependent variable in the ANOVA, and the influences of two independent variables, organ and tag, were tested for significance. The interaction between these two factors (organ and tag) was the focus of our analysis. To visualize differences in normalized tag proportions between organs, the least-square means and 95% confidence limits were plotted for each tag and shown separately by organ using Prism 5 (GraphPad Software).

For the nonmetric multidimensional scaling (nMDS) and principal components analysis (PCA) studies, the quantity of each tag was again normalized and expressed as a proportion of total tags in each sample. Raw data were imported into the multivariate statistical software package Primer 6 (PRIMER-E) and used to calculate Pielou's evenness index $J' =$

H′/H′Max, where H′ represents the Shannon diversity index and H′Max represents the maximum value the index would take given a completely even distribution of *n* number of variables. The evenness measurements for the controls and experimental samples were plotted and analyzed in Prism 5. Normalized tag proportions were imported into primer 6 for PCA using standard methods. The plot of the samples for the first two components is shown in the graph on the *x* and *y* planes, and the loadings of each Eigen vector and Eigen value are reported in Table 1 and 2.

The normalized tag proportions were compared to the proportion of each tag in the inoculum according to the formula $|I_n\text{-}O_n|$ where n equals unique tag, I_n equals the input proportion of tag number n, and O_n equals the output proportion of tag n. This generated a new set of variables that measure the total amount of divergence for a given organ compared to the input mixture of tags. By comparing the distance away from the input, organs from different experiments with different input mixtures could be directly compared provided they contained the same number of tags. The normalized distance measure was imported into Primer 6 and used to create a similarity matrix using the Euclidean distance measure. The similarity matrix was then used in the nMDS application of Primer 6 using 100 iterative restarts. The best scoring ordination of the 100 runs, determined by having the lowest Kruskal stress value, was selected for inclusion in the analysis. Data from CBA/J mice, tested from mixtures of 7 tags, were analyzed separately from control and C57/Bl6 mice, which used the same mixture of 10 tags.

REFERENCES

1. **Griebling TL.** 2005. Urologic diseases in America project: trends in resource use for urinary tract infections in women. J. Urol. **173**:1281–1287.
2. **Litwin MS, et al.** 2005. Urologic diseases in America project: analytical methods and Principal findings. J. Urol. **173**:933–937.
3. **Foxman B.** 2002. Epidemiology of urinary tract infections: incidence, morbidity, and economic costs. Am. J. Med. **113**:5–13.
4. **Zhang L, Foxman B.** 2003. Molecular epidemiology of *Escherichia coli* mediated urinary tract infections. Front. Biosci. **8**:235–244.
5. **Russo TA, Stapleton A, Wenderoth S, Hooton TM, Stamm WE.** 1995. Chromosomal restriction fragment length polymorphism analysis of *Escherichia coli* strains causing recurrent urinary tract infections in young women. J. Infect. Dis. **172**:440–445.
6. **Manges AR, et al.** 2001. Widespread distribution of urinary tract infections caused by a multidrug-resistant *Escherichia coli* clonal group. N. Engl J. Med. **345**:1007–1013.
7. **Foxman B, et al.** 2002. Uropathogenic *Escherichia coli* are more likely than commensal *E. coli* to be shared between heterosexual sex partners. Am. J. Epidemiol. **156**:1133–1140.
8. **Johnson JR, Delavari P.** 2002. Concurrent fecal colonization with extraintestinal pathogenic *Escherichia coli* in a homosexual man with recurrent urinary tract infection and in his male sex partner. Clin. Infect. Dis. **35**:E65–E68.
9. **Johnson JR, Clabots C.** 2006. Sharing of virulent *Escherichia coli* clones among household members of a woman with acute cystitis. Clin. Infect. Dis. **43**:e101–e108.
10. **Bacheller CD, Bernstein JM.** 1997. Urinary tract infections. Med. Clin. North Am. **81**:719–730.
11. **Kaper JB, Nataro JP, Mobley HL.** 2004. Pathogenic *Escherichia coli*. Nat. Rev. Microbiol. **2**:123–140.
12. **Faro S, Fenner DE.** 1998. Urinary tract infections. Clin. Obstet. Gynecol. **41**:744–754.
13. **Anderson GG, et al.** 2003. Intracellular bacterial biofilm-like pods in urinary tract infections. Science **301**:105–107.
14. **Rosen DA, Hooton TM, Stamm WE, Humphrey PA, Hultgren SJ.** 2007. Detection of intracellular bacterial communities in human urinary tract infection. PLoS Med. **4**:e329.
15. **Lane MC, Alteri CJ, Smith SN, Mobley HL.** 2007. Expression of flagella is coincident with uropathogenic *Escherichia coli* ascension to the upper urinary tract. Proc. Natl. Acad. Sci. U. S. A. **104**:16669–16674.
16. **Lane MC, et al.** 2005. Role of motility in the colonization of uropathogenic *Escherichia coli* in the urinary tract. Infect. Immun. **73**:7644–7656.
17. **Wright KJ, Seed PC, Hultgren SJ.** 2005. Uropathogenic *Escherichia coli* flagella aid in efficient urinary tract colonization. Infect. Immun. **73**: 7657–7668.
18. **Snyder JA, et al.** 2004. Transcriptome of uropathogenic *Escherichia coli* during urinary tract infection. Infect. Immun. **72**:6373–6381.
19. **Hagan EC, Lloyd AL, Rasko DA, Faerber GJ, Mobley HL.** 2010. *Escherichia coli* global gene expression in urine from women with urinary tract infection. PLoS Pathog. **6**:e1001187.
20. **Craig NL.** 1991. Tn*7*: a target site-specific transposon. Mol. Microbiol. **5**:2569–2573.
21. **Peters JE, Craig NL.** 2001. Tn*7*: smarter than we thought. Nat. Rev. Mol. Cell Biol. **2**:806–814.
22. **Waterston RH, et al.** 2002. Initial sequencing and comparative analysis of the mouse genome. Nature **420**:520–562.
23. **Hagan EC, Mobley HL.** 2008. Haem acquisition is facilitated by a novel receptor Hma and required by uropathogenic *Escherichia coli* for kidney infection. Mol. Microbiol. **71**:79–91.
24. **Johnson DE, et al.** 1998. Comparison of *Escherichia coli* strains recovered from human cystitis and pyelonephritis infections in transurethrally challenged mice. Infect. Immun. **66**:3059–3065.
25. **Johnson JR, et al.** 2005. The IrgA homologue adhesin Iha is an *Escherichia coli* virulence factor in murine urinary tract infection. Infect. Immun. **73**:965–971.
26. **Sabri M, Houle S, Dozois CM.** 2009. Roles of the extraintestinal pathogenic *Escherichia coli* ZnuACB and ZupT zinc transporters during urinary tract infection. Infect. Immun. **77**:1155–1164.
27. **Schwartz DJ, Chen SL, Hultgren SJ, Seed PC.** 2011. Population dynamics and niche distribution of uropathogenic *E. coli* during acute and chronic urinary tract infection. Infect. Immun. **79**:4250–4259.
28. **Gransden WR, Eykyn SJ, Phillips I, Rowe B.** 1990. Bacteremia due to *Escherichia coli*: a study of 861 episodes. Rev. Infect. Dis. **12**:1008–1018.
29. **Levins R.** 1969. Some demographic and genetic consequences of environmental heterogeneity for biological control. Bull. Entomol. Soc. Am. **15**: 237–240.
30. **Hanski I.** 1998. Metapopulation dynamics. Nature **396**:41–49.
31. **Aronson M, Medalia O, Amichay D, Nativ O.** 1988. Endotoxin-induced shedding of viable uroepithelial cells is an antimicrobial defense mechanism. Infect. Immun. **56**:1615–1617.
32. **Mulvey MA, et al.** 1998. Induction and evasion of host defenses by type 1-piliated uropathogenic *Escherichia coli*. Science **282**:1494–1497.
33. **Orikasa S, Hinman F, Jr..** 1977. Reaction of the vesical wall to bacterial penetration: resistance to attachment, desquamation, and leukocytic activity. Invest. Urol. **15**:185–193.
34. **Haraoka M, et al.** 1999. Neutrophil recruitment and resistance to urinary tract infection. J. Infect. Dis. **180**:1220–1229.
35. **Valore EV, et al.** 1998. Human beta-defensin-1: an antimicrobial peptide of urogenital tissues. J. Clin. Invest. **101**:1633–1642.
36. **Abraham JM, Freitag CS, Clements JR, Eisenstein BI.** 1985. An invertible element of DNA controls phase variation of type 1 fimbriae of *Escherichia coli*. Proc. Natl. Acad. Sci. U. S. A. **82**:5724–5727.
37. **Gunther NW, Lockatell V, Johnson DE, Mobley HL.** 2001. *In vivo* dynamics of type 1 fimbria regulation in uropathogenic *Escherichia coli* during experimental urinary tract infection. Infect. Immun. **69**: 2838–2846.
38. **Mobley HL, et al.** 1990. Pyelonephritogenic *Escherichia coli* and killing of cultured human renal proximal tubular epithelial cells: role of hemolysin in some strains. Infect. Immun. **58**:1281–1289.
39. **Mobley HL, et al.** 1993. Isogenic P-fimbrial deletion mutants of pyelonephritogenic *Escherichia coli*: the role of alpha Gal(1–4) beta Gal binding in virulence of a wild-type strain. Mol. Microbiol. **10**:143–155.
40. **de Lorenzo V, Herrero M, Jakubzik U, Timmis KN.** 1990. Mini-Tn5 transposon derivatives for insertion mutagenesis, promoter probing, and chromosomal insertion of cloned DNA in gram-negative eubacteria. J. Bacteriol. **172**:6568–6572.
41. **Redford P, Welch RA.** 2006. Role of sigma E-regulated genes in *Escherichia coli* uropathogenesis. Infect. Immun. **74**:4030–4038.
42. **Bao Y, Lies DP, Fu H, Roberts GP.** 1991. An improved Tn*7*-based system for the single-copy insertion of cloned genes into chromosomes of gram-negative bacteria. Gene **109**:167–168.
43. **Sambrook J, Fritsch EF, Maniatis T.** 1989. Molecular cloning: a laboratory manual, 2nd ed. Cold Spring HarborLaboratory Press, Cold Spring Harbor, NY.
44. **Hagberg L, et al.** 1983. Ascending, unobstructed urinary tract infection in mice caused by pyelonephritogenic *Escherichia coli* of human origin. Infect. Immun. **40**:273–283.